V European Conference on Computational Fluid Dynamics
ECCOMAS CFD 2010
J. C. F. Pereira and A. Sequeira (Eds)
Lisbon, Portugal, 14–17 June 2010

COMPARISON OF THREE NONLINEAR MODELS TO ANALYZE WAVE PROPAGATION OVER SUBMERGED TRAPEZOIDAL BREAKWATERS

Teixeira P.R.F.[*], Pinheiro L.[†], Fortes C.M.J.[††]

[*]Universidade Federal do Rio Grande – FURG
Av. Itália, km 8, Campus Carreiros, 96201-900, Rio Grande, RS, Brasil
e-mail: pauloteixeira@furg.br

[††]Laboratório Nacional de Engenharia Civil
Av. do Brasil, 101, 1700-066, Lisboa, Portugal

e-mail: lpinheiro@lnec.pt, jfortes@lnec.pt

Key words: Numerical simulation, Wave propagation, Breakwaters, Boussinesq

Abstract. *The main objective of this paper is to evaluate the capabilities of three numerical models to simulate wave propagation over submerged trapezoidal breakwaters. These models differ both in the nonlinearity level and the numerical methods: (a) BOUSS3W, which is a Boussinesq type finite element model, that solves the extended Boussinesq equations derived by Nwogu; (b) COULWAVE, which is a finite difference model that solves the nonlinear equations of Boussinesq presented by Wei et al., considering a multi-layer concept; (c) FLUINCO, which solves the Navier-Stokes equations discretized in time and space through a semi-implicit two-step Taylor-Galerkin method. Whereas the two first models are vertically integrated, the third is not, so it can capture the vertical profile of the velocity. BOUSS3W presents good linear wave characteristics up to kh~3, while the second-order nonlinear behaviour is well-captured up to kh~1. COULWAVE exhibits accurate linear characteristics up to kh~8 and nonlinear accuracy up to kh~6. Moreover, in the first model, equations are deduced using the velocity at an arbitrary distance from the still water level, while the second one considers the vertical flow field approximated by a quadratic polynomial at each layer in which the water column is divided. Two case studies were simulated. In the first breakwater, downstream and upstream slopes are equal to 1:10 and 1:20, respectively. In the second breakwater, both downstream and upstream slopes are equal to 1:2. Numerical results are compared with experimental ones in terms of surface elevation and energy spectrum distribution at various points. Streamline distribution obtained by FLUINCO are presented, showing the influence of vertical circulation on the behavior of the surface elevation. In general, results for weakly nonlinear cases are similar among models, but for highly nonlinear cases, the code FLUINCO has presented better results because of its vertical discretization.*

1 INTRODUCTION

Waves experiment significant transformation in shape, height, direction and velocity when they propagate from deep to shallow waters. Refraction, diffraction, reflection, breaking, and other non linear phenomena associated with wave-wave and wave-current interaction are some causes of these modifications.

The numerical models based on Boussinesq equations have been adopted to simulate typical non linear coastal engineering problems in the last decades. Examples of these types of models are BOUSS3W (BOUSSinesq model with Internal Irregular Wave generation) [1] and COULWAVE [2].

BOUSS3W, that is valid from intermediate to shallow waters, solves the extended Boussinesq equations deduced by Nwogu [3]. A type of velocity profile in a pre-defined depth is assumed to the vertical integration of the equations. The model can simulate non linear and dispersive propagation of regular and irregular waves, including some of the most important phenomena that occur in the coastal regions. It uses the SPRINT package [4] for the temporal integration and the Galerkin method with a non structured mesh of finite elements for spatial discretization.

COULWAVE is a finite difference model that solves the fully non linear and dispersive Boussinesq equations. Lynett and Liu used the multi-layer concept in which the water column is divided by several layers. The accuracy depends on the numbers of layers enabling simulations in deep waters.

COULWAVE exhibits accurate linear characteristics up to kh~8 and nonlinear accuracy up to kh~6, while BOUSS3W only presents linear wave characteristics up to kh~3, and the second-order nonlinear behaviour is well-captured up to kh~1. Moreover, COULWAVE can simulate more wave transformation phenomena compared to BOUSS3W such as refraction (due to the current), run-up and run-down. However, BOUSS3W model presents higher potential to simulate wave propagation in 2DH regions such as in harbour regions or in irregular closed boundary zones. In fact, firstly, the computational domain can be discretized with a finite element mesh better adapted to irregular areas and secondly, it considers different partial reflection conditions along the boundaries of the computational domain, thus, simulating different structures and boundary types that can occur in harbours. On the other hand, COULWAVE does not consider the partial reflection condition.

Models based on the integration of the Navier-Stokes equations, initially developed in hydrodynamic areas, enable an accurate simulation of the wave transformations in small coastal regions. Teixeira [5] has developed a code, named FLUINCO, which uses a fractioned method to simulate 3D incompressible fluid flow problems with free surface. It uses the two-step semi implicit Taylor Galerkin method to discretize the Navier-Stokes equations in time and in space. A linear tetrahedral element that has the advantage to adapt to complex geometry domains and a good computational efficiency is adopted. An arbitrary lagrangean eulerian (ALE) formulation is employed to solve problems with large relative movements among bodies and surfaces and free surface movements. The spatial distribution of the mesh velocity minimizes the element distortions using functions that consider the influence of the velocity of each node belonging to the boundary surfaces.

Whatever the numerical model characteristics, the simulation of wave propagation over submerged breakwaters are important tests to validate wave propagation models. In these cases, the harmonic generation [8,9] and the vortex formation, depending on the geometry [10], also occur. When waves propagate in deep waters over a submerged obstacle, part of the wave energy is transferred from the primary wave component to their harmonics, contributing to increase non linearity. Harmonic generation phenomena

that occur when waves propagate over obstacles, such as natural reefs, were studied theoretically [11], experimentally [6,7,12] and numerically [7,12,13,14,15,16,17,18]. In some situations, the correct simulation of the flow can only be figured out considering the viscosity effects [19]. Huang and Dong [10] studied the interaction between solitary waves and rectangular submerged breakwaters using a model based on 2D Navier-Stokes equations and concluded that the flow around the breakwater is laminar, without turbulence. The experimental studies carried out by Ting and Kim [19] and Zhuang and Lee [20] show that velocity fluctuations do not exist around the breakwater.

Wave propagations over two types of trapezoidal breakwaters are studied in this paper. In the first case, which is studied experimentally by Dingemans [6], downstream and upstream slopes are 1:20 and 1:10, respectively. In the second one that is analyzed by Ohyama et al. [7] both downstream and upstream slopes are 1:2.

Chapter 2 describes the numerical models BOUSS3W, COULWAVE and FLUINCO whereas Chapter 3 shows the numerical simulation for wave propagation over two types of breakwaters. Finally, Chapter 4 presents the conclusion of this paper.

2 NUMERICAL MODELS

2.1 BOUSS3W model

BOUSS3W solves the extended Boussinesq equations deduced by Nwogu [3] as follows:

$$\frac{\partial \mathbf{u}}{\partial t}+(\mathbf{u}\cdot\nabla)\mathbf{u}+g\nabla\eta+\frac{Z_\alpha^{\,2}}{2}\nabla\left(\nabla\cdot\frac{\partial \mathbf{u}}{\partial t}\right)+Z_\alpha\nabla\left(\nabla\cdot\left(h\frac{\partial \mathbf{u}}{\partial t}\right)\right)=n\,f_l\,\mathbf{u}+n\,f_t\,\mathbf{u}|\mathbf{u}|+\frac{1}{h+\eta}\left(f_w\mathbf{u}|\mathbf{u}|+\nabla\upsilon\nabla((h+\eta)\mathbf{u})\right), \quad (1)$$

$$\frac{\partial \eta}{\partial t}+\nabla((h+\eta)\mathbf{u})+\nabla\cdot\left(\left(\frac{Z_\alpha^{\,2}}{2}-\frac{h^2}{6}\right)h\nabla(\nabla\cdot\mathbf{u})+\left(Z_\alpha+\frac{h}{2}\right)h\nabla(\nabla\cdot(h\mathbf{u}))\right)=S_f+\upsilon_s\nabla\eta, \quad (2)$$

where the velocity vector $\mathbf{u}=\mathbf{u}(x,y,t)=(u,v)$ is the bi-dimensional velocity field, calculated in the depth Z_α, $\eta=\eta(x,y,t)$ is the free surface elevation, h is the depth and g is the gravity acceleration. The terms on the right hand side of the equations are added terms to the original equations to take into account: partial reflection and transmission trough porous structures (where: n is the porosity, f_l, f_t are the laminar and turbulent friction factors), energy dissipation due to bottom friction and wave breaking (where f_w is the bottom friction factor and υ is the eddy viscosity due to breaking waves), the wave generation inside the domain using a source function (where S_f is the source function) and a viscous term (where υ_s is the viscosity) used to control numerical instabilities and to absorb outgoing waves in sponge layers placed at the fully absorbing boundaries.

The model uses SPRINT package [4] for the temporal integration. This software employs a general method to solve ordinary partial differential equation systems using both suitable time steps and variable integration order. In bi-dimensional cases, the jacobian matrix is factorized because it is sparse.

The Galerkin method with a non structured mesh of finite elements is used for spatial discretization. This mesh is generated through an automatic generator GMALHA [21], developed exclusively for wave propagation models.

Regular or irregular waves can be generated using the source function condition [22]. Total or partial reflection as well as total absorption are the boundary conditions implemented in the model.

2.2 COULWAVE model

COULWAVE [2] is a finite difference model to simulate strong non linear (the relation between the wave amplitude and the depth is up to 1) and dispersive wave propagation in variable depth zones. The continuity and momentum Boussinesq equations are integrated along the depth by using a multi-layer concept. A velocity profile for each layer, coincident in the boundary between neighboring layers, is assumed. Therefore, these equation systems enable the applicability of the model to be extended for deep water, simulating linear characteristics up to kh~8 and second order non linear behavior up to kh~6. Mass conservation and momentum equations for one layer can be expressed by:

$$\begin{aligned}&\frac{1}{\varepsilon_o}\frac{\partial h}{\partial t}+\frac{\partial \varsigma}{\partial t}+\nabla.[(\varepsilon_o\varsigma+h)\mathrm{u}_1]\\&-\mu_o{}^2\nabla.\left\{\left[\frac{\varepsilon_o^3\zeta^3+h^3}{6}-\frac{(\varepsilon_o\zeta\ +h)k_1^2}{2}\right]\nabla(\nabla.\mathrm{u}_1)+\left[\frac{\varepsilon_o^2\zeta^2-h^2}{2}-(\varepsilon_o\zeta\ +h)k_1\right]\nabla T_1\right\}=O(\mu_o^4)\end{aligned} \tag{3}$$

$$\begin{aligned}&\frac{\partial \mathrm{u}_1}{\partial t}+\varepsilon_o\,\mathrm{u}_1.\nabla\mathrm{u}_1+\nabla\varsigma+\mu_o^2\frac{\partial}{\partial t}\left\{\frac{k_1^2}{2}\nabla(\nabla.\mathrm{u}_1)+k_1\nabla T_1\right\}+\varepsilon\mu_o^2\begin{bmatrix}(\mathrm{u}_1.\nabla k_1)\nabla T_1+k_1\nabla(\mathrm{u}_1.\nabla T_1)+k_1(\mathrm{u}_1.\nabla k_1)\nabla(\nabla.\mathrm{u}_1)\\+\frac{k_1^2}{2}\nabla(\mathrm{u}_1.\nabla(\nabla.\mathrm{u}_1))\end{bmatrix}\\&+\varepsilon_o\mu_o^2\left[T_1\nabla T_1-\nabla\left(\varsigma\frac{\partial T_1}{\partial t}\right)\right]+\varepsilon_o^2\mu_o^2\nabla\left(\varsigma\,S_1T_1-\frac{\varsigma^2}{2}\frac{\partial(\nabla.\mathrm{u}_1)}{\partial t}-\varsigma\,\mathrm{u}_1.\nabla T_1\right)+\varepsilon_o^3\mu_o^2\nabla\left[\frac{\varsigma^2}{2}\left((\nabla.\mathrm{u}_1)^2-\mathrm{u}_1.\nabla(\nabla.\mathrm{u}_1)\right)\right]=O(\mu_o^4)\end{aligned} \tag{4}$$

where

$$T_1=\nabla.(h\mathrm{u}_1)+\frac{1}{\varepsilon_o}\frac{\partial h}{\partial t}\quad;\quad k_1=\alpha_1 h+\beta_1\varsigma\quad;\quad \varepsilon_o=\frac{a_o}{h_o}\quad;\quad \mu_o=\frac{h_o}{l_o}.$$

ζ is the free surface elevation, h is the depth, $\boldsymbol{u}_1$ is the horizontal velocity vector in the depth defined in each layer and g is the gravity acceleration. α_1 and β_1 coefficients are defined by users, a_o is the wave amplitude, h_o is the depth and l_o is the wavelength. The horizontal velocity of the vertical profile is given by:

$$U_1=u_1-\mu_o^2\left\{\frac{z_1^2-k_1^2}{2}\nabla(\nabla.u_1)+(z_1-k_1)\nabla T_1\right\}+O(\mu_o^4) \tag{5}$$

where Nwogu [3] suggests z_1 = -0.531h.

The solution for these equations is similar to the formulation presented by Wei et al. [22] that use the Adams-Bashforth predictor-corrector scheme. The finite difference scheme consists in the explicit 3rd order Adams-Bashforth scheme for the predictor step, and the implicit 4th order one for the corrector step in time. The central finite difference with accuracy of the 4th order is used for first order spatial derivates. The superior order for spatial and temporal derivates has second order accuracy, through three-point central schemes. The model has accuracy up to Δt^4 in time and up to Δx^4 in space.

Two types of boundary conditions are applied: total reflection and radiation. For the former, Wei et al.'s [22] methodology is used while for the latter, sponge layer according to Kirby et al. [23] is employed.

Lynett and Liu [2,24] added other terms to the equations to consider the bottom friction, breaking waves and wave generation in the interior of the domain.

2.3 FLUINCO model

Basically, the algorithm consists in the following steps [25]:

(a) Calculate non-corrected velocity at $\Delta t/2$, where the pressure term is at t instant, according to Eq. (6).

$$\tilde{U}_i^{n+1/2} = U_i^n - \frac{\Delta t}{2}\left(\frac{\partial f_{ij}^n}{\partial x_j} - \frac{\partial \tau_{ij}^n}{\partial x_j} + \frac{\partial p^n}{\partial x_i} - w_j^n \frac{\partial U_i^n}{\partial x_i}\right) \quad (i,j=1,2,3)\ , \tag{6}$$

where ρ is the specific mass, p is the pressure, $U_i = \rho \mathrm{v}_i$, $f_{ij} = \mathrm{v}_j(\rho \mathrm{v}_i) = \mathrm{v}_j U_i$, v_i are the velocity components, w_i are the velocity components of the reference system and τ_{ij} is the viscous stress tensor (i,j =1,2,3).

(b) Update the dynamic pressure p at $t+\Delta t$, given by the Poisson equation:

$$\frac{1}{c^2}\Delta p = -\Delta t\left[\frac{\partial \tilde{U}_i^{n+1/2}}{\partial x_i} - \frac{\Delta t}{4}\frac{\partial}{\partial x_i}\frac{\partial \Delta p}{\partial x_i}\right] \quad (i = 1,2,3)\ . \tag{7}$$

where $\Delta p = p^{n+1} - p^n$.

(c) Correct the velocity at $t+\Delta t/2$, adding the pressure variation term from t to $t+\Delta t/2$, according to the equation:

$$U_i^{n+1/2} = U_i^n - \frac{\Delta t}{2}\left(\frac{\partial f_{ij}^n}{\partial x_j} - \frac{\partial \tau_{ij}^n}{\partial x_j} + \frac{\partial p^n}{\partial x_i} + \frac{1}{2}\frac{\partial \Delta p}{\partial x_i} - w_j^n \frac{\partial U_i^n}{\partial x_i}\right) \quad (i,j=1,2,3)\ , \tag{8}$$

(d) Calculate the velocity at $t+\Delta t$ using variables updated in the previous steps as follows:

$$U_i^{n+1} = U_i^n - \Delta t\left(\frac{\partial f_{ij}^{n+1/2}}{\partial x_j} - \frac{\partial \tau_{ij}^{n+1/2}}{\partial x_j} + \frac{\partial p^{n+1/2}}{\partial x_i} - w_j^{n+1/2}\frac{\partial U_i^{n+1/2}}{\partial x_i}\right) \quad (i,j=1,2,3). \tag{9}$$

The standard Galerkin weighted residual method is applied to discretize Eq. (6) to (9) in space, using a tetrahedra element. A constant shape function is used for variables at $t+\Delta t/2$, while a linear shape function is employed at t and $t+\Delta t$.

FLUINCO model assumes the free surface subjected to a constant atmospheric pressure (normally, the reference value is null) and imposes the free surface kinematic boundary condition (KBC), using the ALE formulation expressed as [26]:

$$\frac{\partial \eta}{\partial t} + \left({}^{(s)}\mathrm{v}_i - {}^{(s)}\mathrm{w}_i\right)\frac{\partial \eta}{\partial x_i} = 0 \quad (i = 1,2,3)\ , \tag{10}$$

where η is the free surface elevation, ${}^{(s)}\mathrm{v}_i$ and ${}^{(s)}\mathrm{w}_i$ are fluid and mesh velocity components in the free surface, respectively. An eulerian formulation is used for x and y direction on the horizontal plane and an ALE formulation is employed to z direction. The temporal discretization of the KBC is made in the same way as in the momentum equations, using triangular elements coincident with faces of the tetrahedra that belong to the free surface.

The spatial distribution of the mesh velocity minimizes the element distortions through the functions that weight the influence of the velocity of each node belonging to surface boundaries.

3 NUMERICAL SIMULATIONS

Two different configurations of the trapezoidal breakwaters, with different level of non-linearity, are used to test the behaviour of the numerical models. In the first case, the downstream and upstream slopes are 1:20 and 1:10, respectively [6]. In the second one, both slopes are 1:2 [7], where the non-linear effects are more significant.

3.1 Breakwater with slopes 1:20 and 1:10

Figure 1 shows the channel and the submerged breakwater geometries, and the position of the gauges. The channel is 23m in length, 0.4m and 0.1m are the maximum and the minimum depths, respectively. In the channel entrance, a monochromatic wave is generated with a period of 2.02s and an amplitude of 0.01m.

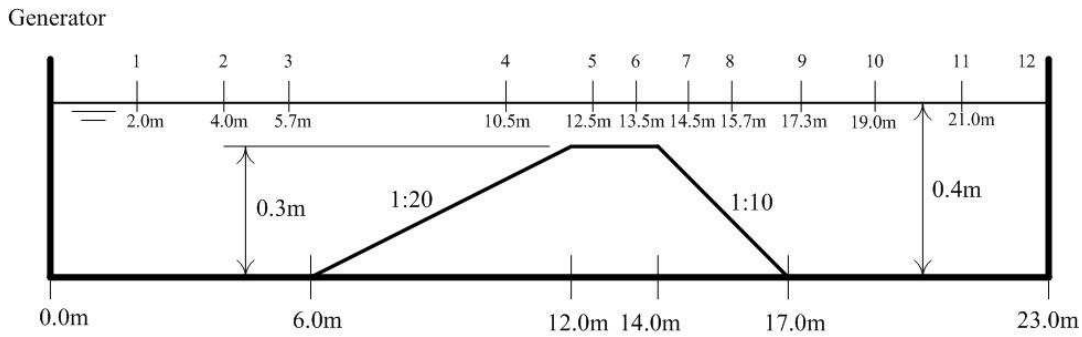

Figure 1: Channel geometry for the 1:20 and 1:10 breakwater

Table 1 presents some parameters for this case study. H/h, even on the platform, has small values in comparison with breaking limit of approximately 0.8 [27]. The case involves intermediate water for the channel ($0.314 < kh < 3.142$) and shallow water for the platform ($kh < 0.314$). Ursell numbers ($Ur = gHT^2/h^2$) show that the non-linear effects on the platform are more intensive.

	H/h	**kh**	**Ur**
Channel (h = 0.4m)	0.050	0.674	5.0
Platform (h = 0.1m)	0.259	0.318	103.6

Table 1: Wave parameters for the 1:20 and 1:10 breakwater

Table 2 presents periods, frequencies and wavelengths concerning the fundamental frequency and the harmonic components that occur along the wave propagation. The wavelength was estimated according to the dispersion equation of the linear theory. These values are references to determine discretizations in time and space to be used in the modeling.

	Fundamental	**2nd harmonic**	**3rd harmonic**	**4th harmonic**
Period (s)	2.02	1.01	0.67	0.50
Frequency (Hz)	0.50	1.00	1.50	2.00
Wavelength (m)	3.73	1.46	0.70	0.39

Table 2: Period, frequency and wavelength concerning the fundamental frequency, and 2nd, 3rd and 4th harmonics for the 1:20 and 1:10 breakwater

The numerical domain used by BOUSS3W is 39m long (23m + 8m on each side to accommodate the two sponge layers and the source function) and its discretization was made by linear finite elements with two nodal points. The grid spacing was $\Delta x = 0.01$m,

which led to 3901 nodes. Wave generation was made using the source function where its centre is situated at x = 8 m and has a width of one wavelength. At both ends, 2 m long sponge layers were placed. A zero initial condition and no diffusion condition were used in this calculation. The calculations were performed during approximately 6000Δt, with Δt = 0.01s, in order to enable the wave field to develop fully in the whole computational domain.

The COULWAVE numerical domain is 32 m long and 1 m wide. The bathymetry was reproduced by discretization using a spacing of Δx = 0.05 m. The COULWAVE model generates a finite difference grid based on the minimum number of points per wavelength given by the user, which in this case was 50. The Courant number was equal to 0.1. Two layers were considered in these calculations. Two absorbing boundaries were considered at the beginning and at the end of the domain with a length of one wavelength. A friction coefficient equal to 1.0×10^{-2} was adopted. The source function for the wave generation is located at x = 0.0m. The total simulation time was 300 s. For the remaining model parameters, the values suggested in the COULWAVE model user's manual [2] were assumed in the first attempt.

FLUINCO used a mesh with 88700 elements and 37296 nodes. Twenty layers of elements were used in vertical direction, where small elements are located near the bottom and the free surface. Along the channel, the element sizes vary from Δx = 0.08m in the boundary to Δx = 0.025m around the platform. In the transversal direction, only one layer of elements is used, because the behavior of the flow is bi-dimensional. In the entrance of the domain, the wave generation condition is imposed while at the end the radiation condition is imposed. The velocity components are null on the bottom and the KBC is imposed in the free surface. The velocity component perpendicular to the surface is null for lateral walls (symmetry condition). As an initial condition, the velocity field is null and the pressure one is hydrostatic. The time step is 0.003s, a fact that satisfies the Courant stability condition.

Figure 2 shows the free surface elevations in gauge 3, located downstream the breakwater (x=5.7m); in gauge 6, on the platform (x=13.5m); in gauge 8, in the middle of the upstream slope (x=15.7m); and in gauge 11, on the upstream and far from the breakwater (x=23m). Results obtained by numerical models are compared with the experimental ones presented by Dingemans [6].

In general, there is good agreement between numerical results and experimental ones in gauges 3 and 6. BOUSS3W showed a slightly higher crest in gauge 3. In gauge 6, FLUINCO presents slightly smooth surface deformation, while BOUSS3W differs a little more in oscillations with higher frequencies. In gauges 8 and 11, corresponding to downstream, the nonlinear effects are more significant. The deformations in gauge 8 are well represented by FLUINCO and COULWAVE. Although the FLUINCO results get closer to the experimental ones in some regions, there are difficulties in representing the deformations related to higher harmonics, possibly due to the lack of an appropriate discretization to capture the nonlinear phenomena. In this gauge, BOUSS3W shows discrepancies both in the shape and in the magnitude of deformations. FLUINCO has a better behavior in relation to the others in gauge 11. COULWAVE shows good results, but differs somewhat in the waves of higher frequencies. On the other hand, BOUSS3W does not represent the phenomenon well, with significant differences compared to other models.

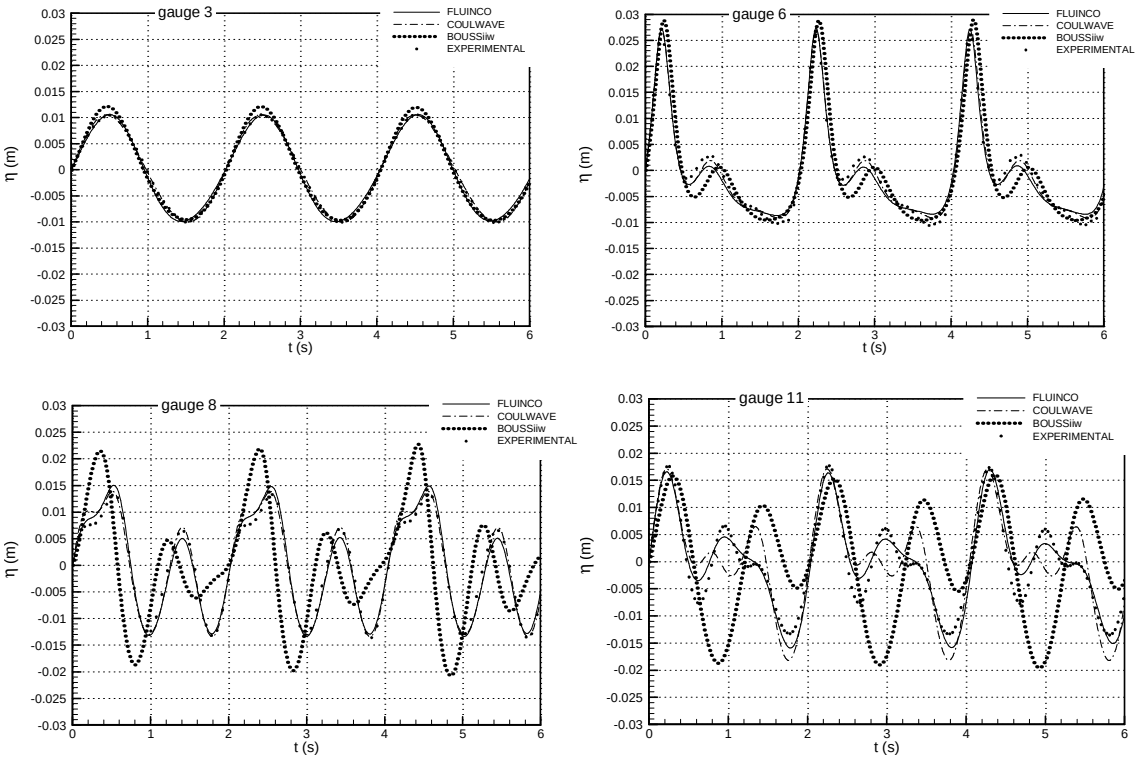

Figure 2: Free surface elevation of the 1:20 and 1:10 breakwater

Figure 3 shows the frequency spectra obtained by models in the gauges and a comparison with the experimental results. The differences found in the free surface elevation are confirmed in Figure 3, which shows differences in the intensity of harmonic components, mainly in gauges located at the end of the channel. The numerical models adequately simulate the position of the peaks of the fundamental frequency and the harmonic components throughout the domain. However, there are some differences in the amplitude of these peaks, especially in gauges 8 and 11. The BOUSS3W model results do not show the presence of the third harmonic in gauge 11, unlike the other models.

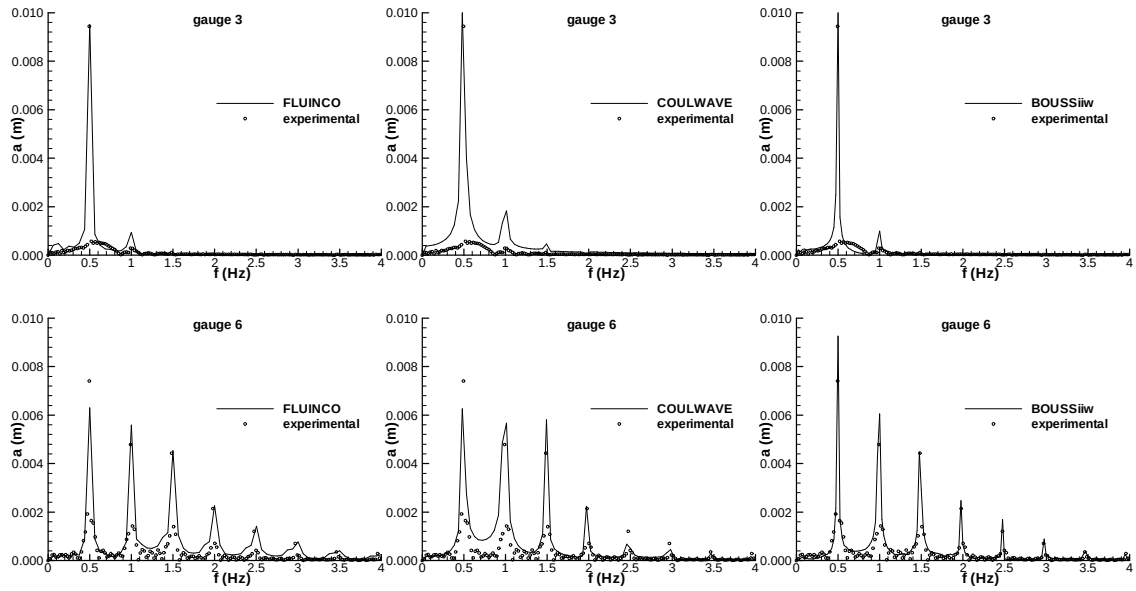

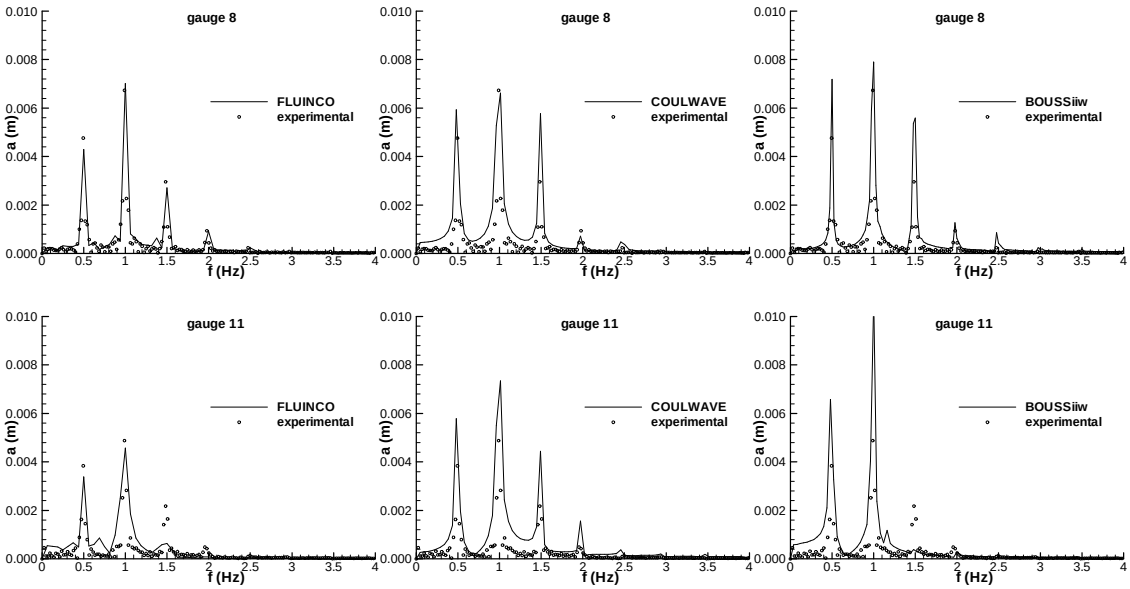

Figure 3: Numerical and experimental frequency spectrum in the gauges of the breakwater 1:20 and 1:10

Figure 4 presents the streamlines around the upstream slope of the breakwater in eleven instants completing one wave period obtained by FLUINCO. We can observe that the flow separation and the vortex do not exist at all instants, due to the mild inclination of the upstream slope.

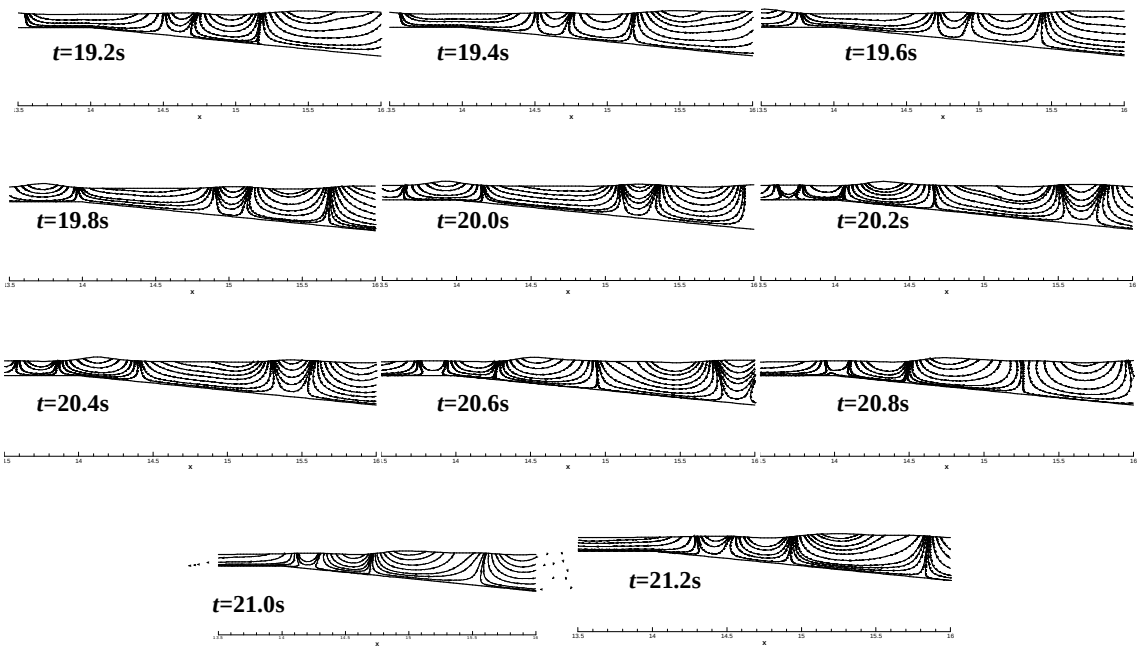

Figure 4: Streamlines of the 1:20 and 1:10 breakwater

3.2 Breakwater with slopes 1:2

In this case, the length of the channel is 35m and the maximum and the minimum depths are 0.5m and 0.15m, respectively (See Fig. 5). In the entrance of the channel, a monochromatic wave is generated with a period of 2.68s, related to a wavelength of 5.66m in the channel, and an amplitude of 0.025m. This problem is case 6 studied by Ohyama et al. [7] who analyzed six different types of waves experimentally. Table 3

shows some parameters that characterize the problem, calculated according to the linear theory. The Ursell number on the platform is 210, indicating the strong non-linearity in this region. Parameter H/h shows that breaking does not even occur on the platform.

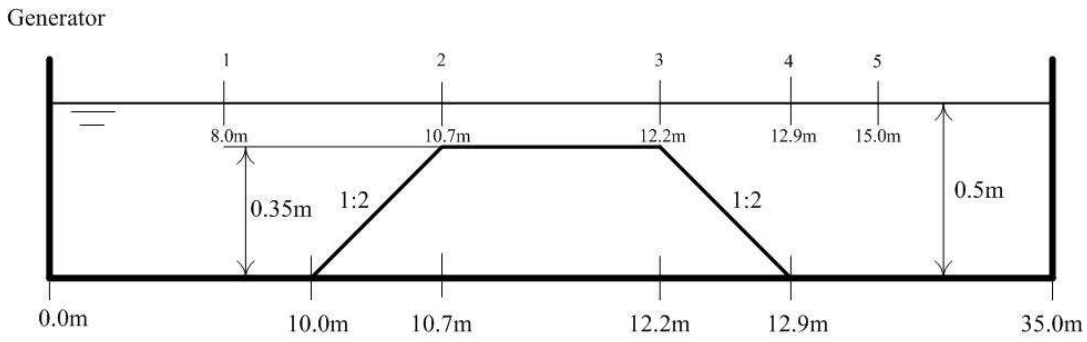

Figure 5: Geometry of the channel for the 1:2 breakwater

	H/h	kh	Ur
Channel (h = 0.5m)	0.100	0.555	14.1
Platform (h = 0.15m)	0.355	0.294	210.0

Table 3: Wave parameters for the 1:2 breakwater

Table 4 shows periods, frequencies and wavelengths concerning the fundamental frequency and the harmonic components that occur along the wave propagation.

The numerical domain used by BOUSS3W is 43m long (35m + 8m on the left side to accommodate the sponge layer and the source function) and its discretization was made by linear finite elements with two nodal points. The grid spacing was $\Delta x = 0.01$m, which led to 4301 nodes. The centre of the source function is situated at x=8 m and has a width of one wavelength. At both ends, 2m long sponge layers were placed. A zero initial condition and no diffusion condition were used in this calculation. The calculations were performed during approximately $6000\Delta t$, with $\Delta t = 0.01$s, in order to enable the wave field to develop fully in the whole computational domain.

The COULWAVE numerical conditions in this case were quite similar to the ones used in section 3.1. A higher number of points per wavelength equal to 70 was considered.

A mesh with 120200 elements and 50526 nodes was used for FLUINCO in this simulation. The element sizes along the channel vary between dx=0.08m at the ends and dx=0.01m on the platform. The boundary and the initial conditions are similar to the ones in the previous case, and 0.002s was the time step.

	Fundamental	2nd harmonic	3rd harmonic	4th harmonic
Period (s)	2.68	1.34	0.89	0.67
Frequency (Hz)	0.373	0.746	1.124	1.493
Wavelength (m)	5.66	2.42	1.22	0.70

Table 4: Period, frequency and wavelength related to the fundamental frequency, and 2nd, 3rd, and 4th harmonics for the 1:2 breakwaters

Figure 6 shows the free surface elevations in gauges 3 and 5 (gauge positions are indicated in Fig. 5). Numerical results are compared with the experimental ones presented by Ohyama et al. [7]. The FLUINCO and the COULWAVE models represent the surface deformation recorded in gauge 3 well, while BOUSS3W presents some numerical oscillations of higher frequency. The deformations of gauge 5 indicate that

the nonlinearity increases. In this case, FLUINCO captures the variation of the surface elevation more accurately. COULWAVE shows some numerical disturbances, but reproduces the experimental results reasonably. Moreover, BOUSS3W presents smooth results, which are different both in the shape and in the magnitude of the deformations.

Figure 7 shows frequency spectra obtained in gauges 3 and 5. The fundamental and the harmonic waves are well represented by the models, but their amplitudes differ. The FLUINCO and the COULWAVE results are closer for the two gauges. There are some differences from those obtained by BOUSS3W, especially in gauge 5, which does not show the presence of the fourth harmonic and the following.

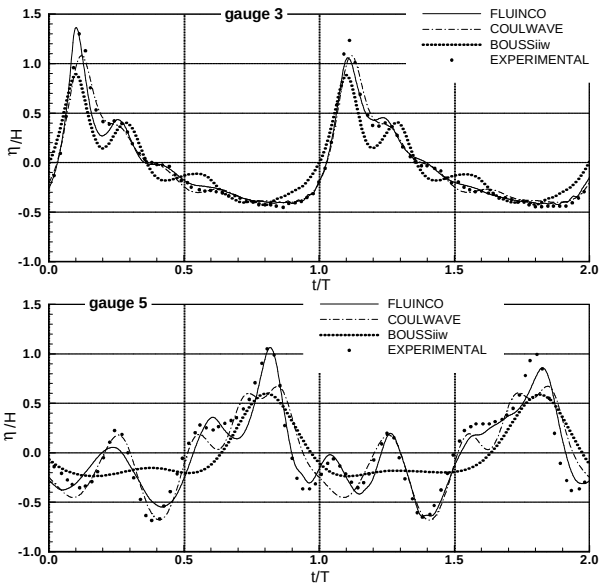

Figure 6: Free surface elevation for the 1:2 breakwater in gauges 3 and 5.

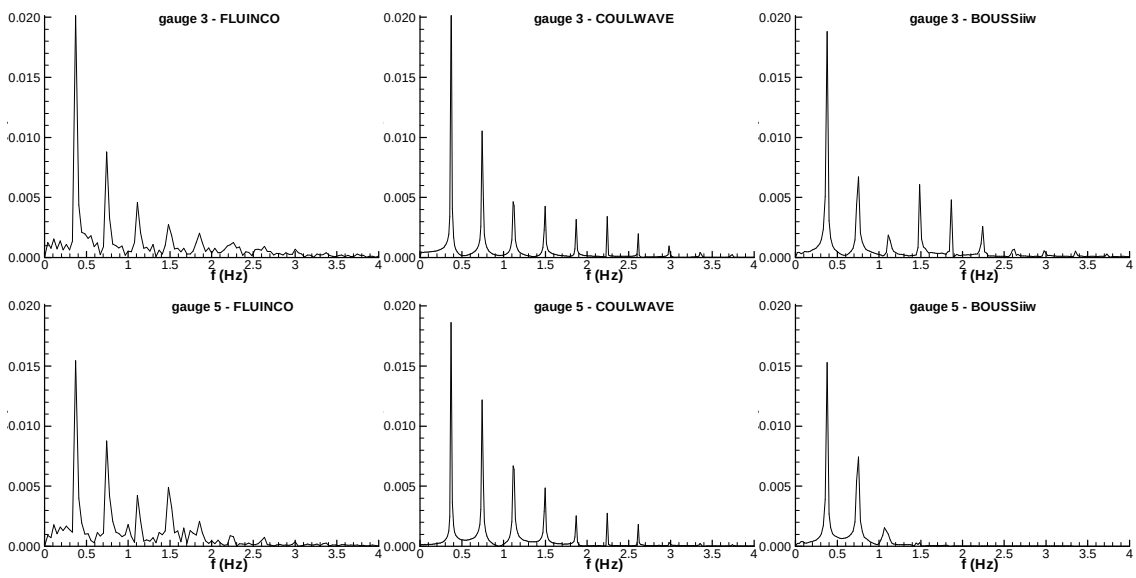

Figure 7: 1:2 Breakwater case. Frequency spectra in gauges 3 and 5.

Streamlines during one wave period obtained by FLUINCO are presented in Fig. 8. Unlike the previous case, a vortex, located between the upstream slope and the bottom, occurred during part of the wave period.

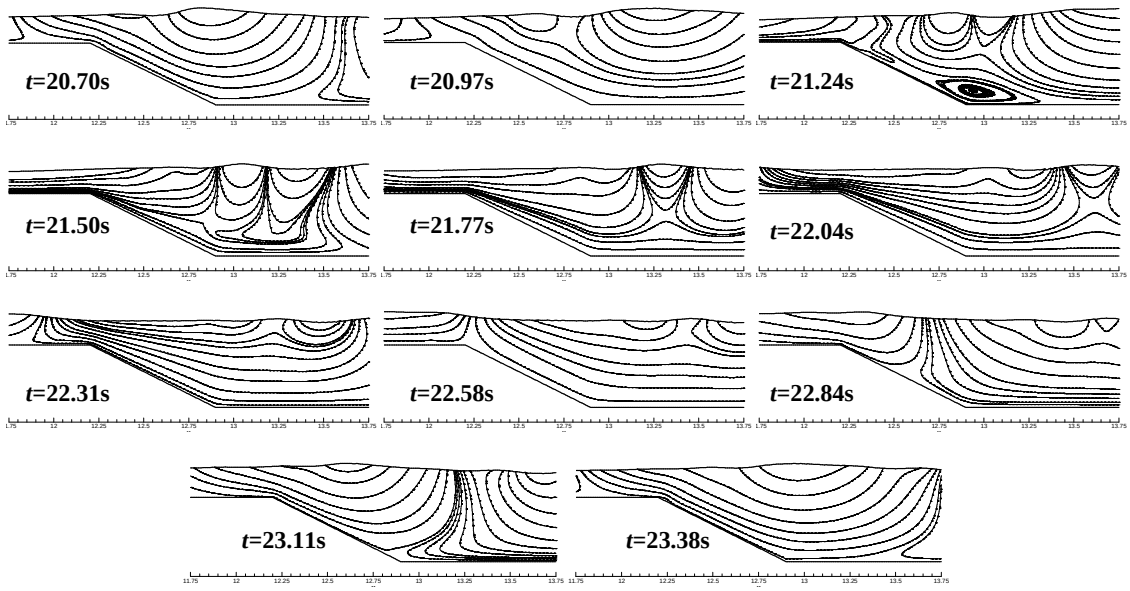

Figure 8: Streamlines of the 1:2 breakwater

4 CONCLUSIONS

Results of three numerical models (FLUINCO, COULWAVE and BOUSS3W) for two cases of trapezoidal breakwaters with different slopes are compared in this paper. While FLUINCO is a model based on the direct integration of the Navier-Stokes equations, COULWAVE and BOUSS3W solve the extended Boussinesq equations.

The first case study deals with upstream and downstream slopes of 1:20 and 1:10, respectively. Its results obtained by the models were compared with Dingemans' experimental data [6]. A comparison of the surface elevations and the energy spectrum for some gauges along the channel showed that the models provided good results. Although the FLUINCO results have been somewhat smoothed, they were closer to the experimental ones, including the ones in the gauges placed on the downstream, where nonlinear effects are more significant. COULWAVE proved to be a robust model, representing the surface deformation adequately even in zones with strong nonlinearity. Moreover, the BOUSS3W model represented the deformations in the upstream of the breakwater well, but there were some differences in the downstream, where high order harmonics were not captured. Streamlines over a wave period obtained by FLUINCO show that there is no flow separation in this case.

The analysis of the 1:2 breakwater slope case showed a strong influence of nonlinear effects on the results of the surface elevation and the energy spectrum. The numerical results were compared with experimental ones presented by Ohyama et al [7]. The vertical velocity field obtained by FLUINCO showed that a vortex of non-turbulent origin was formed in the flow. FLUINCO obtained results closer to the experimental ones, including the ones in the downstream of the breakwater, where the nonlinearity effects are more significant. COULWAVE presented a good behavior, with some numerical oscillations of higher frequency in the downstream regions. The numerical disturbance presented by BOUSS3W is intensified in the downstream zones, where the shape of the surface deformations was not adequately represented.

The two cases showed that FLUINCO captures the nonlinear effects of the flow more accurately, due to the fact that this model considers the influence of the vertical circulation in the flow, unlike the Boussinesq models (COULWAVE and BOUSS3W). They also indicated better robustness of COULWAVE compared with BOUSS3W, possibly due to the higher order nonlinear terms included in the Boussinesq equations.

On the other hand, FLUINCO consumes more computational time that justifies the use of Boussinesq models in which the vertical movement does not influence the flow behavior significantly.

AKNOWLEDGMENT

This paper was developed in the partnership between LNEC and FURG. This study is funded by the FCT project PTDC/ECM/67411/2006 and by the CAPES project EPDE/0857/08-4.

REFERENCES

[1] L. Pinheiro, Um método de elementos finitos para a discretização das equações de Boussinesq estendidas. Tese de mestrado. Engenharia Mecânica, IST (2007)

[2] P. Lynett and P.L-F Liu, Modelling wave generation, evolution and interaction with Depth-Integrated, Dispersive Wave equations. COULWAVE Code Manual. Cornell Univ. Long Inter. Wave Modelling Package (2004)

[3] O. Nwogu, Alternative form of Boussinesq equations for near-shore wave propagation. *J. Waterway, Port, Coastal, and Ocean Engineering* **119** (6), pp. 618-638 (1993)

[4] M. Berzins, R.M. Furzeland and L.E. Scales, A user's manual for SPRINT - a versatile software package for solving systems of algebraic, ordinary and partial differential equations: Part 3 - advanced use of SPRINT. Technical Report TNER.85.058, Thornton Res. C, Chester (1985)

[5] P.R.F. Teixeira, Simulação numérica da interação de escoamentos tridimensionais de fluídos compressíveis e incompressíveis e estruturas deformáveis usando o método de elementos finitos. Porto Alegre. Tese de doutorado, PPGEC-UFRGS, (2001)

[6] M.W. Dingemans, Comparison of computations with Boussinesq-like models and laboratory measurements. Report H-1684.12 Delft Hydraulics, 32 pp, (1994)

[7] T. Ohyama, W. Kioka and A. Tada, Applicability of numerical models to nonlinear dispersive waves. *Coastal Engrg.* **24**, pp. 297-313 (1995)

[8] J.W. Johnson, R.A. Fuchs and J.R. Morison, The damping action of submerged breakwaters. *Trans. Am. Geophys. Union* **32**, pp.704-718 (1951)

[9] P. Jolas, Passage de la houle sur un seuil. *Houille Blanche* **2**, pp.148-152 (1960)

[10] C.J. Huang and C.M. Dong, Wave deformation and vortex generation in water waves propagating over a submerged dike. *Coastal Engrg*. **37**, pp.123-148 (1999)

[11] D.H. Peregrine, Long waves on a beach. *J. Fluid Mech*. **27**, pp.815-882 (1967)

[12] S. Beji and J. A. Battjes, Experimental investigations of wave propagation over a bar", *Coastal Engineering* **19**, pp. 151-162 (1993)

[13] J.G. Zhou and P.K. Stansby, An arbitrary Lagrangian-Eulerian σ (ALES) model

with non-hydrostatic pressure for shallow water flows. *Comput. Meth. Appl. Mech. Eng.* **178**, pp.199-214 (1999)

[14] P. Lin and C.W. Li, A σ-coordinate three-dimensional numerical model for surface wave propagation. *Int. J. Numer. Meth. Fluids* **38**, pp.1045-1068 (2002)

[15] V. Casulli and G.S. Stelling, G.S., Numerical simulation of 3D quasi-hydrostatic, free-surface flows. *J. Hydr. Eng. ASCE* **124**, pp.678-686 (1998)

[16] H.L. Yuan and C.H. Wu, A two-dimensional vertical non-hydrostatic σ model with an implicit method for free-surface flows. *Int. J. Numer. Meth. Fluids* **44**, pp.811-835 (2004)

[17] G.S. Stelling and M. Zijlema, Further experience in computing non-hydrostatic free-surface flow involving with water waves. *Int. J. Numer. Meth. Fluids* **48**, pp.169-197 (2005)

[18] Y.M. Shen, C.O. Ng and Y.H. Zheng, Simulation of wave propagation over a submerged bar using the VOF method with a two-equation k-epsilon turbulence modeling. Ocean Eng. **31**, pp.87-95 (2004).

[19] F.C.K. Ting and Y.K. Kim, Vortex generation in water-waves propagating over a submerged obstacle. *Coast. Eng.* 24, pp.23-49 (1994)

[20] F. Zhuang and J.J. Lee, A viscous rotational model for wave overtopping over marine structure. *Proc. 25th Int. Conf. Coastal Eng. ASCE*, pp. 2178-2191 (1996)

[21] L. Pinheiro, J.L.M. Fernandes and C.J.E.M. Fortes, Finite Element Mesh Generator with Local Density Conditioned to Bathymetry for Wave Propagation Models in Coastal Zones. Proc. of EUA4X@IAC 06, Roma Italy, October 2006. IMACS Series in *Comp. and Applied Mathematics* **12**, pp. 71-80 (2007)

[22] G. Wei, J.T. Kirby and A. Sinha, Generations of waves in Boussinesq models using a source function method, *Coastal Eng.* **36** (4), pp. 271-299 (1999)

[23] J.T. Kirby, G. Wei, Q. Chen, A.B. Kennedy and R.A. Dalrymple, FUNWAVE 1.0 – Fully Nonlinear Boussinesq Wave Model Documentation and User's Manual, Res. Rep. No.CACR 98-06 (1998)

[24] P. Lynett and P.L-F Liu, A two-layer approach to water wave modelling. *Proceedings of the Royal Society of London A* **460**, pp. 2637– 2669 (2004)

[25] P.R.F. Teixeira and A.M. Awruch, Numerical simulation of three dimensional incompressible flows using the finite element method. *ENCIT*, (8), Porto Alegre (2000)

[26] R. Ramaswamy and M. Kawahara, Arbitrary lagrangian-eulerian finite element method for unsteady, convective, incompressible viscous free surface fluid flow. *International Journal for Numerical Methods in Fluids.* **(7)**, pp. 1053-1075 (1987)

[27] R.G. Dean and R.A. Dalrymple, Water Wave Mechanics for Engineers and Scientists, In: Advanced Series on Ocean Engineering **2**, World Scientific Publishing Co. Ltd. (1994)